Journal of Advanced Research in Applied Sciences and Engineering Technology

Journal homepage:
https://semarakilmu.com.my/journals/index.php/applied_sciences_eng_tech/index
ISSN: 2462-1943

Preparation and Characterization of a Clay-Based Ceramic Membrane for Tannery Wastewater Treatment

Muazu Abubakar[1,*], Norhayati Ahmad[2]

[1] Department of Mechanical Engineering, Bayero University Kano, PMB 3011 Nigeria
[2] Faculty of Mechanical Engineering, Universiti Teknologi Malaysia, 81310 Johor Bahru, Malaysia

ARTICLE INFO

Article history:
Received 23 December 2022
Received in revised form 16 January 2023
Accepted 7 February 2023
Available online 1 March 2023

Keywords:
Montmorillonite; Mesoporous; Membrane; Tannery wastewater

ABSTRACT

In this work, a porous clay-based ceramic membrane was developed from locally sourced clay from Nigeria. The clay was ground and sieved through 100 µm size. The chemical, mineralogical, thermal and particle size properties of the clay were determined using XRF, XRD, TGA/DTA and PSD respectively. Starch composition from 10-25 wt% was added to the clay and thoroughly mixed with water. The dough was cast on a potter's wheel. The produced membranes were fired at a temperature of 900 °C. The maturation properties of the fired clay were determined using bulk density and apparent porosity. Multi-point BET was used to determine the pore characteristics of the membranes. The flexural strength of the produced membrane was determined using a three-point bending test. The microstructure of the fired clay was recorded using FESEM. Membranes produced from the clay were used for the treatment of tannery wastewater. The XRF result shows that the clay contains high silica and alumina. Also, the XRD results show the clay contains many peaks of montmorillonite and other peaks of feldspar and quartz. The BET shows that the pore size of the membranes produced was in the mesoporous range. From water quality test, it shows that the locally sourced clay can be used to produce ceramic membranes for filtration and separation applications.

1. Introduction

Recently, traditional clay minerals have been successfully used in the production of membranes for the treatment of both industrial and surface wastewater [1]. This arises due to the highly expensive nature of engineering ceramics and the limitations of polymer-based membranes in terms of poor mechanical, thermal and chemical properties [2-8]. In addition, clay-based ceramics have some mechanical properties at par with their engineering ceramics counterparts.

Many researchers have used clay minerals in the fabrication of inexpensive ceramic membranes for wastewater treatment. These membranes were reported to be both macro-porous and meso-porous sizes. For example, Khemakhem *et al.,* [9] reported the development of a membrane using Tunisian clay materials; the pore size of the membrane developed was in the range 5.9-12.8 µm. In

* *Corresponding author.*
E-mail address: amuazu.mec@buk.edu.ng

https://doi.org/10.37934/araset.30.1.114

another research, Nandi *et al.,* [10] conducted work on the development of a clay-based membrane; an average pore size of 0.285 µm was reported. Furthermore, Jana *et al.,* [11], studied the preparation and characterization of low-cost ceramic microfiltration membrane; a pore size in the range of 1.91-4.68 µm was reported. In addition, Vasanth *et al.,* [12] studied the fabrication and properties of a low-cost ceramic membrane from clay for pore sizes in the range 0.5-2.7µm was achieved. In another study, Vasanth *et al.,* [13] studied the development of low-cost membrane from clay an average pore size of 1.32 µm was reported. Years later, BET analysis was employed to study the detailed pore structure of low-cost membranes from clay. For example, Abubakar *et al.,* [14] studied the development of an inexpensive clay membrane from Nigeria; a mesoporous membrane with pore size in the range 5.116.5-6.59 nm was reported. In a similar work, Abubakar *et al.,* [5] studied the effect of milling time on the performance of membranes from ball clay were mesoporous membranes with pore sizes in the range 23.56-38.86 nm.

Several works have reported the use of traditional clays for the development of porous ceramic membranes for filtration, purification and separation applications with excellent densification properties. As the densification properties of porous materials showed their maturation after firing. Researchers reported bulk density and apparent porosity of clay-based porous ceramics in the ranges of 1.52-2.11 g/cm^3 and 23.5-41.45% respectively [7,14,15]. Other properties found in clay-based porous ceramics are relatively good mechanical properties in the range 6.76-17.87 MPa [14,16]. In this study, clay-based porous ceramic was developed using a potter's wheel to achieve a dimensionally uniform porous structure. Nigeria has abundant clay deposits in Africa. However, not many studies have reported the development of porous membranes using clay from Nigeria for the treatment of tannery wastewater. The objective of this work is to develop a clay-based membrane and characterize the membrane as a potential candidate for the treatment of tannery wastewater.

2. Methodology

2.1 Raw Material Preparation and Characterization

The clay used in this research was obtained from Dawakin Kudu, Kano State, Nigeria. The clay was crushed, ground and sieved through a 100 µm sieve with the aid of alumina balls. The particle size distribution of the sieved clay was determined using Malvern mastersizer instrument. The oxide composition of the clay after sieving through 100 µm size sieve was determined using X-ray fluorescence Philips PW 2400. X-ray diffraction was performed on both the clay sieved to 100 µm and the fired clay at a temperature of 900°C with a Cu Kα radiation source with 2θ angle range 4-75° with Empyrean XRD machine. In addition, the thermal behavior of the clay was carried out using thermogravimetric and thermal differential analysis TGA/DTA. The morphology of the clay and the starch were recorded using FESEM (Gemini Supra™35vp).

2.2 Membrane Preparation and Characterization

The clay was mixed with water and a proportionate amount of starch (10, 15, 20 and 25 wt%) was added and mixed thoroughly. The membranes were prepared from this mixture on a potter's wheel through the throwing method. The samples with 10, 15, 20 and 25 wt% starch were labeled as A, B, C and D respectively. The prepared samples were fired at a temperature of 900 °C in an electric furnace Norbetherm to obtain samples with average dimensions of 4 mm height and 60 mm length cm bottom diameter, 15mm. In addition, the XRD of the fired sample at 900°C was conducted using the same Empyrean XRD machine. The FESEM morphology of the fired samples was recorded using

the same Gemini Supra™35vp. The bulk density (BD) and apparent porosity (AP) were determined according to ASTM (1999a) [17]:

$$BD = \frac{W_1}{W_3 - W_2} \times \rho \quad (1)$$

$$AP = \frac{W_3 - W_1}{W_3 - W_2} \times 100 \quad (2)$$

where W_1 is the dry mass of the porous specimen, W_3 is the mass of the porous specimen soaked in water, W_2 is the mass of the porous specimen immersed in water and ρ is the density of water at room temperature.

The flexural strength of the fired samples was determined using three-point bending strength using universal testing machine P5030 Cussons UK at a loading rate of 0.5 mm/min, according to the following equation (ASTM C674-88) [18]:

$$\sigma = \frac{3PL}{Wt^2} \quad (3)$$

where P is the load, L is the span (40mm), w is the width (15 mm) and t is the section thickness of the specimen (4 mm).

2.3 Pore Size Analysis

The adsorption/desorption isotherm, pore size distribution and pore-specific surface area were determined using Surfer BET analyzer, Thermo Scientific. The samples were initially degassed at 150°C for 2 hours after which N_2 was the adsorbate at -196°C for 4 h in a vacuum condition.

2.4 Tannery Wastewater Treatment

To test the potential of the clay as a filter, the clay mixed with the various starch compositions was molded into pot shaped structures. The wastewater obtained from tannery effluent was poured into each of the pots. The filtrate was collected from each of the membranes. The pots prepared and the filtration setup is shown in Figure 1.

The wastewater was characterized using Atomic absorption spectroscopy (AAS), pH, COD, BOD, electrical conductivity (ES) and TSS. Two litres of the wastewater were poured into each of the four pots fired with starch composition 10, 15, 20 and 25 wt%. The permeated water was tested for the water quality parameter (AAS, pH, COD, BOD, ES and TSS).

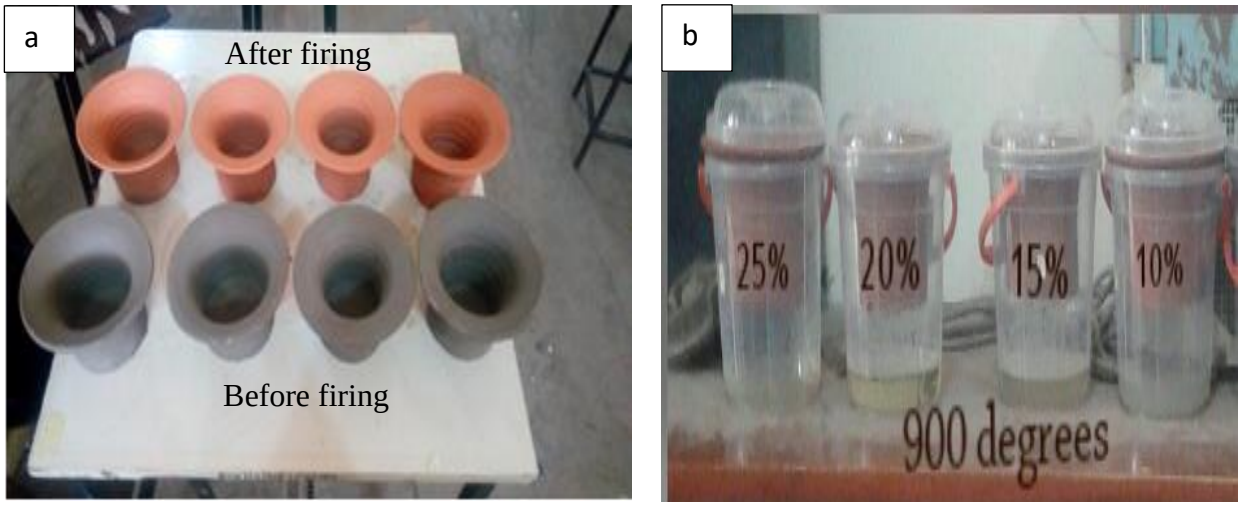

Fig. 1. Pots produced from clay (a) before and after firing and (b) filtration setup

3. Results

3.1 Clay Characteristics

The particle size and cumulative distribution of the clay sieved through 100 µm sieve is shown in Figure 2, which shows a unimodal distribution of the clay particles. In addition, Table 1 shows the summary of the clay properties with a density of 2.36 g/cm^3, a specific area of 0.23 m^2/g and a mean particle size of 30.20 µm. Also, other sizes of the clay D(v, 0.1) shows that only 10% of the particles are below 7.60 µm and D(v, 0.9) shows that 90 % of the particles are below 75.84 µm.

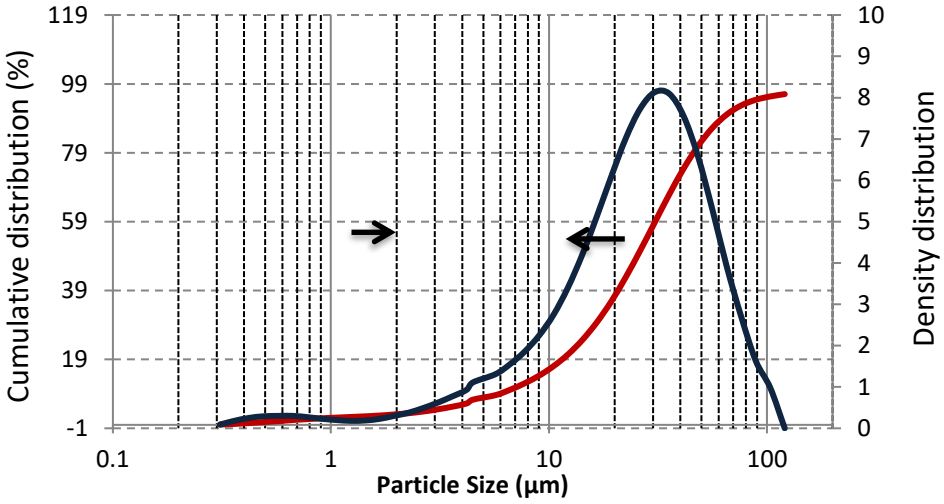

Fig. 2. PSD analysis of clay sieved through 100 µm sieve

The chemical composition analysis (Table 1) shows the clay has higher percentage of constituents of silica and alumina of 46.33 and 36.37 wt% respectively. Other impurities such as Fe_2O_3, MgO, K_2O, CaO and ZrO_2 are present in the clay. Relative high Fe_2O_3 content in the clay since it's the common impurity found in clays as reported by literature [19,20].

Table 1
Chemical and mineralogical analysis of bentonite clay

Compound	% composition by mass of clay	Mineralogy (%)	
SiO_2	46.33	Montmorillonite	78
Al_2O_3	36.37	Quartz	15
Fe_2O_3	6.27	Feldspar	7
MgO	0.87	Plasticity	28
K_2O	0.73	Density ($g/cm^{3)}$	2.36
CaO	0.19	Specific surface area ($m^2/g^{)}$	0.23
ZrO_2	0.05		
LOI	9.19		

The morphology of the bentonite clay and cassava starch used as pore former is shown in Figure 3. From the figure, it shows the presence of montmorilonite sheets which are flat and rigid with face-face interactions binding the sheets together. A similar observation was reported by Huang *et al.,* [21]. The morphology of the cassava starch shows granules of the starch.

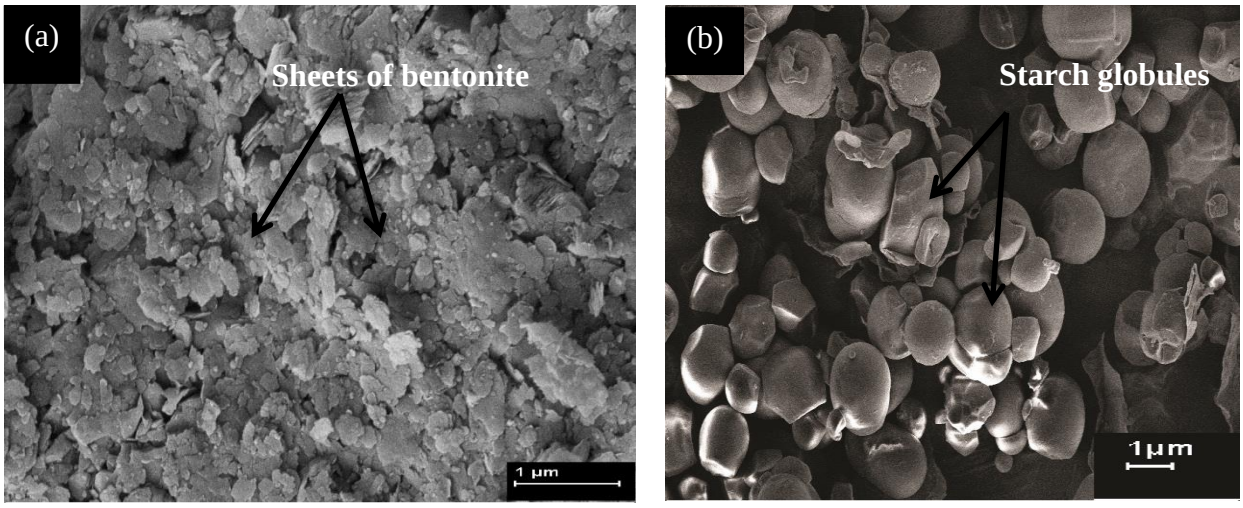

Fig. 3. FESEM of (a) clay and (b) starch

3.2 X-ray Diffraction Analysis of Raw and Fired Clay

The XRD analysis of the raw clay sieved through 100 µm sieve is shown in Figure 4. The figure shows the presence of sharp peaks of montmorillonite and quartz. Also, a feldspar phase is present as shown by a small peak in the figure. This characteristic of the clay is similar to the observations of [22,23]. In the fired clay at 900°C, it shows diminishing peaks of montmorillonite phase, which resulted in the increased intensity of the quartz phase as a result of montmorillonite decomposition [23]. Other properties of the clay are given in Table 1.

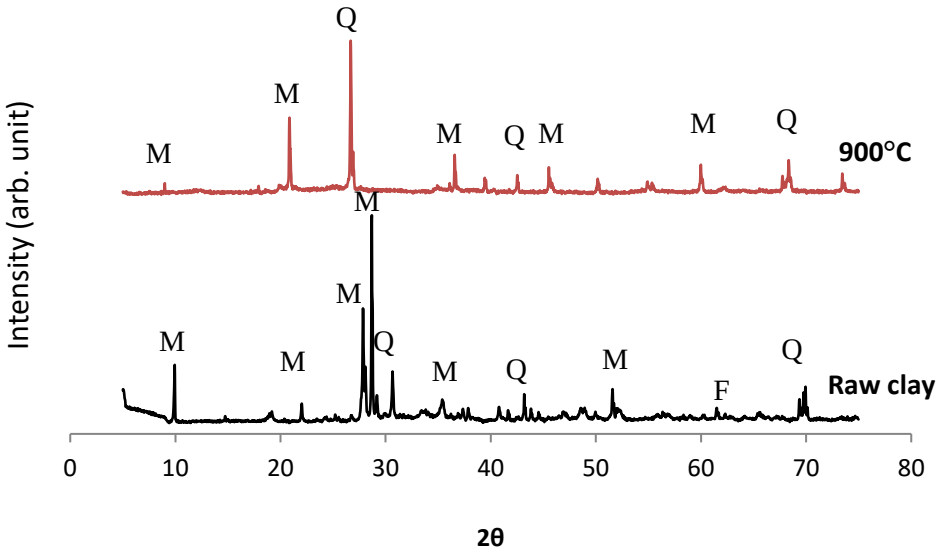

Fig. 4. XRD of raw clay and fired clay at 900°C; M=montmorillonite; Q=Quartz; F=feldspar

3.3 Thermal Analysis

The thermal analysis of the clay through TGA/DTA is shown in Figure 5. From the figure, it shows the various reactions undergone by the clay during heating. The first reaction, which is endothermic at a temperature range 90-110 °C is due to the removal of hygroscopic water in the clay. Another endothermic at temperatures 370 °C is due to the de-hydroxylation of montmorillonite. The DTA also provides information on the heating cycle to which the clay will be subjected to avoid cracking of the pots during firing [24,27]. The TGA analysis shows a total decrease in mass of 3.97% which is due to the removal of hygroscopic water, chemically combined water and other volatile materials present in the clay. Thermal analysis by TGA/DTA is conducted on clays in order to design the heating cycle during firing of the clay to avoid cracking. As clays normally contains physical combine water, chemical combine water and other volatile materials.

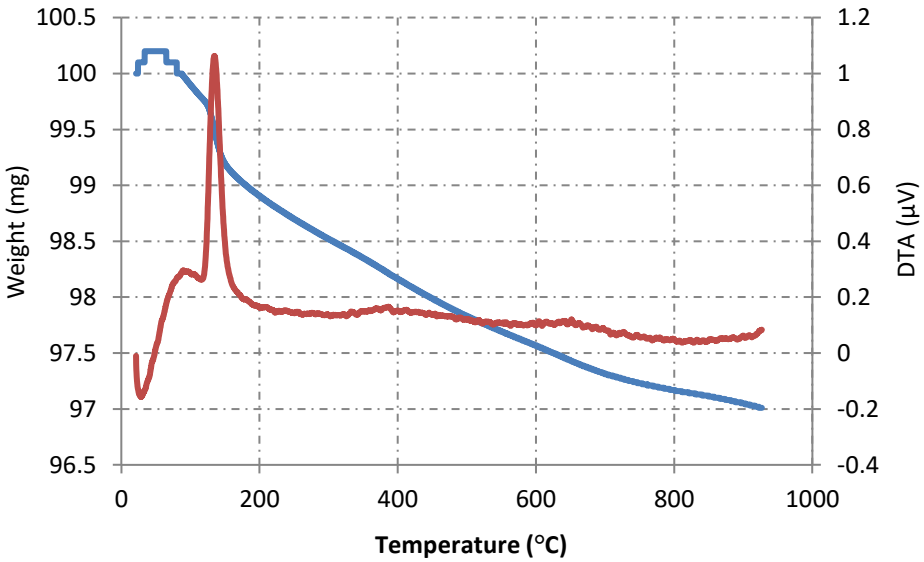

Fig. 5. TGA/DTA analysis of bentonite clay

3.4 FESEM Morphology of the Porous Membrane

The morphology of specimens A, B, C and D fired at 900°C is shown in Figure 6. From the figure, it shows pockets of relatively rounded pores in specimen A. Likewise, Figure 6(b) shows the morphology of the sample with 15 wt% starch, which shows the porosity formed is relatively rounded in shape (slit pores). Figure 6(c) and Figure 6(d) show the presence of interconnected pores in their morphology; this is a result of the starch content, which makes the single slit pores coalesce due to the burn out of the starch at a firing temperature of 900 °C. The microstructures seem to open up due to the increasing amount of starch burn-out as its content increases. An increase in starch to ceramic products increases their porosity after firing [5,14].

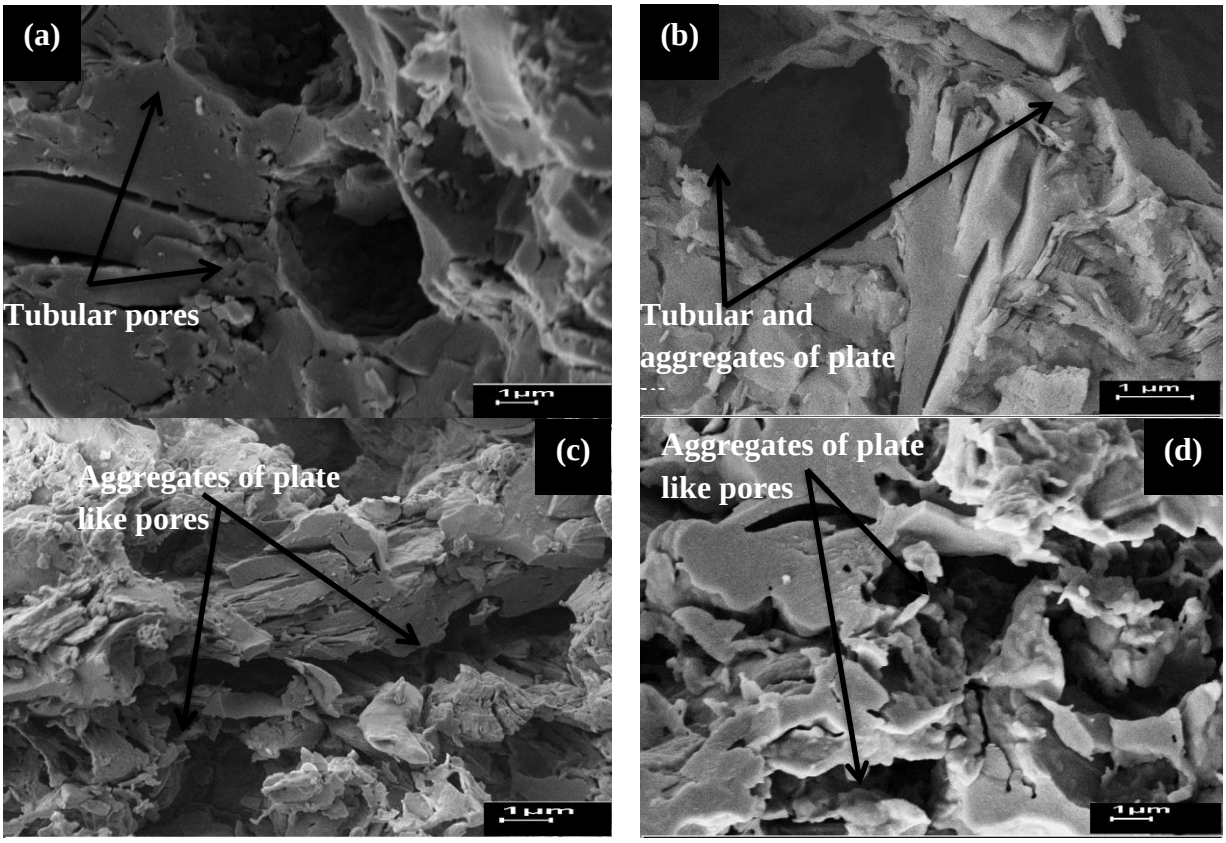

Fig. 6. Fesem of sample (a) A (b) B (c) C and (d) D fired at 900°C

3.5 Flexural Strength

The flexural strength of the porous fired clay (A, B, C and D) at 900 °C is shown in Figure 7. From the figure, it shows that as the percentage of starch increases, the flexural strength decreases. This is a result of an increase in starch content, which during firing at 900 °C will burn out and leave pores as shown in Figure 6. As the percentage of starch increases, the pore created by the starch burnout coalesce and form continuous pores/aggregate plate-like pores (Figure 5(b) to Figure 5(d)), which serve as a crack initiation site and as a result decrease the strength of the porous membranes. A similar observation was reported by Abubakar *et al.,* [14].

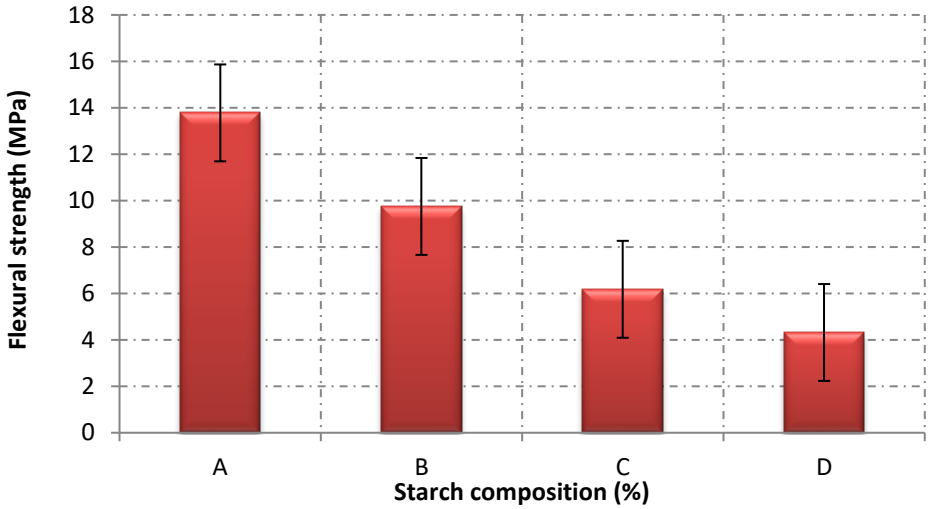

Fig. 7. Flexural strength of sample A, B, C and D fired at 900°C

3.6 Bulk Density and Apparent Porosity

The change of bulk density and apparent porosity against starch content (Figure 8) shows that as percentage starch increases the bulk density decreases at a firing temperature of 900 °C. However, as percentage starch increases the apparent porosity increases. The decrease in bulk density with percentage starch can be attributed to the voids created as the starch burnt out at a firing temperature of 900 °C, which reduces the densification of the membranes. While the increase in porosity as a percentage of starch increase can be due to an increase in the number of pores as the starch burnt out at 900 °C (Figure 6(a) to Figure 6(d)). The starch acted as a pore former in the produced membranes, which at a higher temperature of firing will burn out and form a pore.

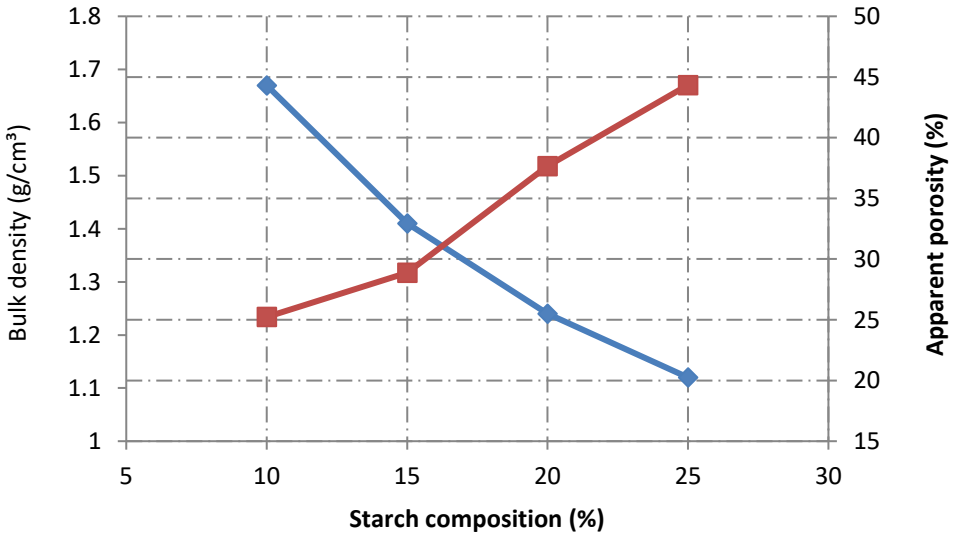

Fig. 8. Bulk density and apparent porosity of A, B, C and D fired at 900°C

3.7 BET Pore Size Analysis

The adsorption/desorption isotherms of the porous samples A, B, C and D are shown in Figure 9. From the figure, it shows sample A has type IV adsorption/desorption isotherm as characterized by hysteresis loop in which the lower adsorption branch is obtained by progressive uptake of nitrogen

gas and the upper desorption branch by the gradual withdrawal of nitrogen gas. Some type IV isotherms are completely reversible. In addition, sample A shows H1 type of hysteresis, which is characteristic of porous materials with cylindrical-like pores (Figure 6(a)). These pores exhibited a narrow distribution in the material. Type H1 hysteresis is characterized by force closure of the hysteresis due to an abrupt drop in volume adsorbed during the desorption process in the relative pressure range of 0.4-0.48. Similarly, samples B, C and D show similar adsorption isotherm patterns. However, the desorption isotherms of B, C and D show similar behavior, which represents type H3 hysteresis. In H3 type hysteresis, the desorption branch is steeper than the adsorption branch, which results in a triangular shape hysteresis loop [25]. H3 hysteresis does not show limiting adsorption at high relative pressure. This behavior is caused by the existence of flexible aggregates of plate-like pores (Figure 6(b) to Figure 6(d)). In general, the presence of hysteresis in adsorption/desorption isotherm suggests that the materials are mesoporous.

The pore size distribution of samples A, B, C and D is also shown in Figure 9. For sample A, it shows a unimodal distribution of the pores, with an average pore size of 20.1 nm. Sample B shows a bimodal distribution of pores with a sharp peak at 1.99 nm and another smaller peak at 25.6 nm. This behavior of sample B can be attributed to the presence of both plate-like pores and cylindrical pores. While samples C and D show unimodal distribution at 37.6 and 40.5 nm respectively. This type of adsorption/desorption isotherm and the pore size ranges show that the membranes produced are mesoporous which has pore sizes in the range 2-50 nm [25,26]. The BET-specific surface area of samples A, B, C and D show an increase with an increase in starch content with values of 15.92, 25.65, 41.54, 51.51 m^2/g respectively. This behavior can be attributed to the increase in starch content, which acted as a pore former in the fired clay at 900°C. A similar observation was reported by Abubakar *et al.,* [14].

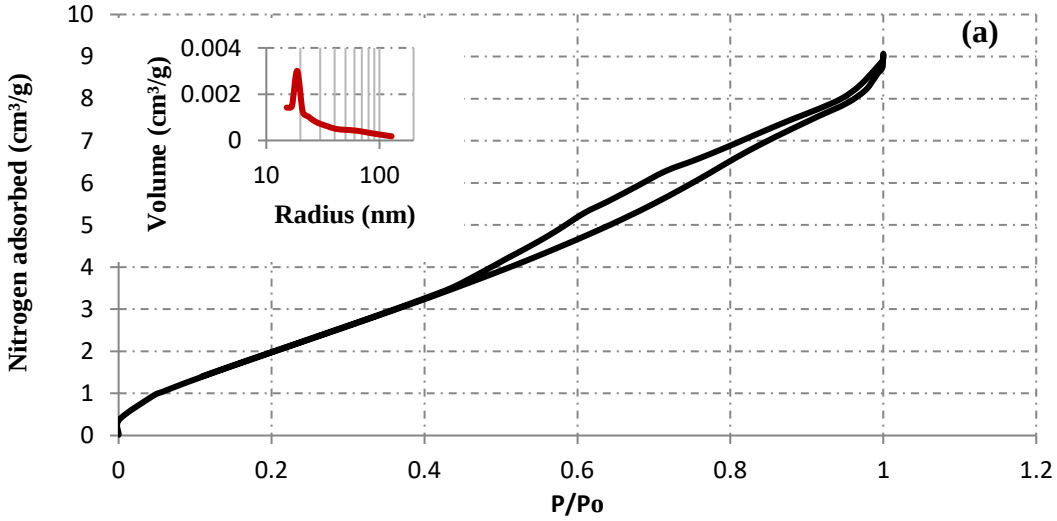

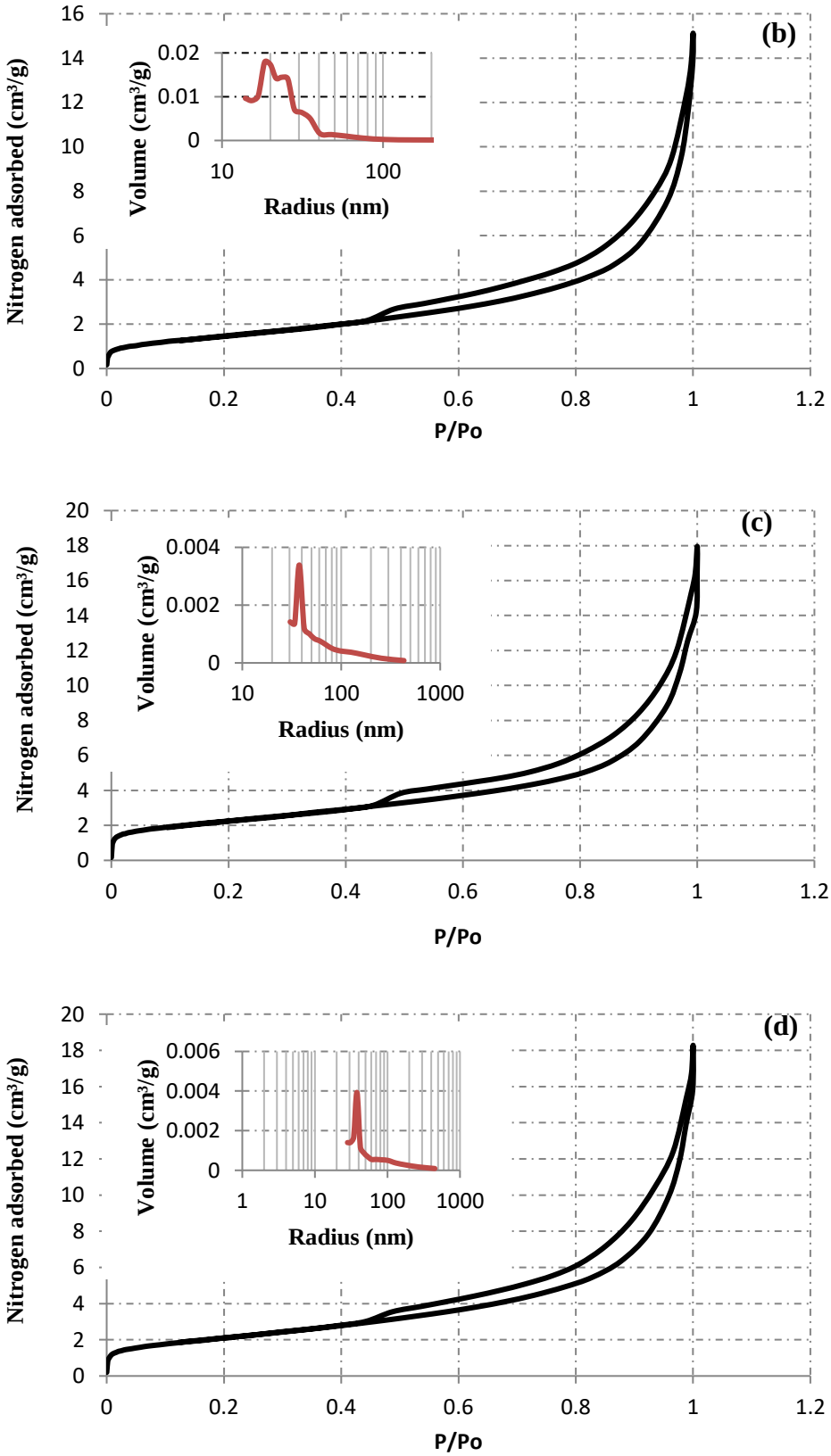

Fig. 9. BET analysis of samples (a) A, (b) B, (c) C and (d) D fired at 900°C

3.8 Water Quality Parameters

The pH value of the wastewater was found to be 10.90, which is far above the pH value recommended for drinking and discharge. After filtration, the pH dropped to 7.4, 7.7, 7.8 and 8 for the membranes with A, B, C and D starch respectively. The pH value for drinking water according to World Health Organization (WHO) should be in the range 6.5-8.5 [27]. Therefore, the wastewater treated with the membranes lies within the WHO recommendations for drinking water. However, the water treated will depend on other water quality testing parameters to meet the standard for drinking.

3.8.1 Total suspended solids (TSS)

The total suspended solids for the value recommended by the raw wastewater and the treated water shows that the TSS for the wastewater is above the value recommended by WHO (810 mg/l) [27]. While the TSS value for the treated wastewater using membranes A, B, C and D are 97, 126, 184 and 205 mg/l respectively. From these values, it shows membranes have performed in reducing the TSS of the wastewater to that recommended by the United States Environmental Protection Agency for drinking water. Figure 10 shows the wastewater from the tannery and the filtrate using pots A, B, C and D.

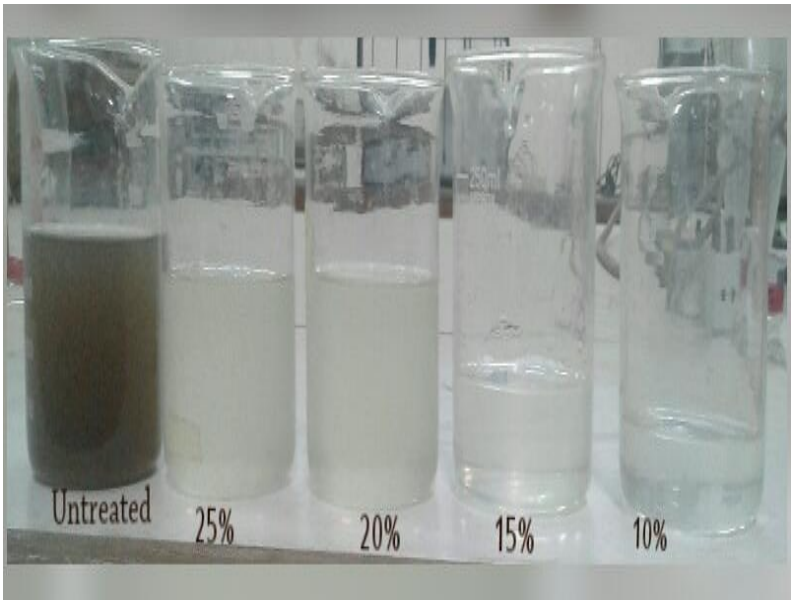

Fig. 10 Tannery wastewater and treated water using membranes A, B, C and D

3.8.2 Electrical conductivity

The electrical conductivity of the tannery wastewater was found to be 3790 us/cm, which is highly above that recommended by Environmental Protection Agency EPA (2500 uc/cm) [28]. The high value of electrical conductivity of the wastewater may be attributed to the salts used during the tanning process, which dissociate into cations and anions, hence, increasing the ionic conductivity of the wastewater. However, after filtration, the filtrate water for membranes A, B, C and D have electrical conductivities of 250, 282, 309 and 321 uc/cm respectively. This may be attributed to the reduction of the cations and anions during the filtration process.

3.8.3 Chemical oxygen demand (COD)

The tannery wastewater has a COD value of 180. The COD of the wastewater shows that it's above the limit recommended by EPA and WHO guidelines of 40. After filtration with membranes A, B, C and D, the COD reduces to 13.50, 34, 44 and 51 respectively.

3.8.4 Chromium concentration

Finally, the chromium concentration in the wastewater shows a value of 4.042 g/cm^3, which is above the value recommended by EPA [28]. Conversely, the chromium content in the filtrate shows values of 0.24, 1.09, 1.97 and 2.13 g/cm^3 respectively. This is in agreement with the electrical conductivity results which show a decrease as chromium will serve as a cation in the wastewater. The chromium content in all the filtrate from the membranes is above that recommended by EPA for drinking water, which is 0.5 g/cm^3. Based on the chromium content in the filtrate the water may not be recommended for drinking, however, the water can be recycled because chromium content above the recommended limit will pose the following health risks skin irritation, skin and nasal ulcers, lung tumors, gastrointestinal effects, damage to the nervous system and circulatory system, accumulates in the spleen, bones, kidney and liver. The major contributors to the worsening pollution of water bodies which lead to above diseases are manufacturing industries, agricultural industries and oil and gas industries [29]. Unfortunately, tannery industries fall under the manufacturing industries contributing to water pollution.

In general, the water quality parameters show a decrease in values as starch content increases in the membranes. This is due to an increase in starch content which acts as a pore former in the membranes. After firing the membranes at 900 °C, the starch will burn out and leave pores. These pores increase in size with an increase in starch content as shown in the FESEM micrographs (Figure 6).

4. Conclusion

A mesoporous clay-based membrane has been developed from locally sourced clay in Nigeria produced on a potter's wheel. In this work the following conclusions can be drawn:

(i) The chemical composition of the clay shows a high percentage of silica and alumina, which are within the range found in bentonite clays.
(ii) The mineralogical composition of the clay shows montmorillonite, quartz and feldspar. These phases are normally found in bentonite clays.
(iii) Membrane properties such as bulk density, flexural strength and shrinkage show a decrease with a percentage increase in starch. However, the apparent porosity shows an increase with an increase in starch content.
(iv) The FESEM morphology of the samples shows the interconnection of pores as the percentage of starch increases.
(v) The adsorption/desorption isotherm shows the presence of hysteresis in the membranes, which is a typical feature of mesoporous materials. In addition, the pore size of the membranes shows to be mesoporous in size.

Acknowledgment
Special acknowledgment to Universiti Teknologi Malaysia through research grants: FRGS 5F421, UTMPR 00L65, CRG 4B537 AND TDR 06G32 for sponsoring some of the laboratory works.

References

[1] Golubenko, D. V., P. A. Yurova, A. V. Desyatov, I. A. Stenina, S. A. Kosarev, and A. B. Yaroslavtsev. "Pore Filled Ion-Conducting Materials Based on Track-Etched Membranes and Sulfonated Polystyrene." *Membranes and Membrane Technologies* 4, no. 6 (2022): 398-403. https://doi.org/10.1134/S2517751622060026

[2] Das, Bipul, Bandana Chakrabarty, and Pranab Barkakati. "Separation of oil from oily wastewater using low cost ceramic membrane." *Korean Journal of Chemical Engineering* 34 (2017): 2559-2569. https://doi.org/10.1007/s11814-017-0185-z

[3] Rawat, Manju, and Vijaya Kumar Bulasara. "Synthesis and characterization of low-cost ceramic membranes from fly ash and kaolin for humic acid separation." *Korean Journal of Chemical Engineering* 35 (2018): 725-733. https://doi.org/10.1007/s11814-017-0316-6

[4] Abubakar, Muazu, and Norhayati Ahmad. "Activity Reduction of 232Th and 40K from Simulated Underground Water Using a Clay-Based Membrane." In *MATEC Web of Conferences*, vol. 203, p. 03003. EDP Sciences, 2018. https://doi.org/10.1051/matecconf/201820303003

[5] Abubakar, Muazu, Siti Fawziah binti Mohd Noor, and Norhayati Ahmad. "Effect of milling time on the performance of ceramic membrane from ball clay for the treatment of nickel plating wastewater." *Journal of the Australian Ceramic Society* 55 (2019): 667-679. https://doi.org/10.1007/s41779-018-0276-2

[6] Abubakar, M., A. Muthuraja, and N. Ahmad. "Experimental investigation of the effect of temperature on the density of kaolin clay." *Materials Today: Proceedings* 41 (2021): 791-794. https://doi.org/10.1016/j.matpr.2020.08.565

[7] Abubakar, Muazu, Ayyankalai Muthuraja, Dipen Kumar Rajak, Norhayati Ahmad, Catalin I. Pruncu, Luciano Lamberti, and Ashwini Kumar. "Influence of firing temperature on the physical, thermal and microstructural properties of kankara kaolin clay: a preliminary investigation." *Materials* 13, no. 8 (2020): 1872. https://doi.org/10.3390/ma13081872

[8] Zaidan, Nurhanna Mohd, Norhayati Ahmad, Yuzo Nakamura, and Muazu Abubakar. "Sayong Ball Clay Membrane for Copper and Nickel Removal from Effluent." *Journal of Advanced Research in Fluid Mechanics and Thermal Sciences* 79, no. 2 (2021): 131-138. https://doi.org/10.37934/arfmts.79.2.131138

[9] Khemakhem, Sabeur, André Larbot, and R. Ben Amar. "New ceramic microfiltration membranes from Tunisian natural materials: application for the cuttlefish effluents treatment." *Ceramics International* 35, no. 1 (2009): 55-61. https://doi.org/10.1016/j.ceramint.2007.09.117

[10] Nandi, B. K., A. Moparthi, R. Uppaluri, and M. K. Purkait. "Treatment of oily wastewater using low cost ceramic membrane: Comparative assessment of pore blocking and artificial neural network models." *Chemical Engineering Research and Design* 88, no. 7 (2010): 881-892. https://doi.org/10.1016/j.cherd.2009.12.005

[11] Jana, Somen, M. K. Purkait, and Kaustubha Mohanty. "Preparation and characterization of low-cost ceramic microfiltration membranes for the removal of chromate from aqueous solutions." *Applied Clay Science* 47, no. 3-4 (2010): 317-324. https://doi.org/10.1016/j.clay.2009.11.036

[12] Vasanth, D., G. Pugazhenthi, and R. Uppaluri. "Fabrication and properties of low cost ceramic microfiltration membranes for separation of oil and bacteria from its solution." *Journal of Membrane Science* 379, no. 1-2 (2011): 154-163. https://doi.org/10.1016/j.memsci.2011.05.050

[13] Vasanth, D., G. Pugazhenthi, and R. Uppaluri. "Biomass assisted microfiltration of chromium (VI) using Baker's yeast by ceramic membrane prepared from low cost raw materials." *Desalination* 285 (2012): 239-244. https://doi.org/10.1016/j.desal.2011.09.055

[14] Abubakar, Muazu, Mohd Nasir Tamin, Muneer Aziz Saleh, M. B. Uday, and Norhayati Ahmad. "Preparation and characterization of a nigerian mesoporous clay-based membrane for uranium removal from underground water." *Ceramics International* 42, no. 7 (2016): 8212-8220. https://doi.org/10.1016/j.ceramint.2016.02.031

[15] Dondi, Michele, Claudio Iglesias, Eduardo Dominguez, Guia Guarini, and Mariarosa Raimondo. "The effect of kaolin properties on their behaviour in ceramic processing as illustrated by a range of kaolins from the Santa Cruz and Chubut Provinces, Patagonia (Argentina)." *Applied Clay Science* 40, no. 1-4 (2008): 143-158. https://doi.org/10.1016/j.clay.2007.07.003

[16] Ngun, Bun Kim, Hasmaliza Mohamad, Shamsul Kamal Sulaiman, Kiyoshi Okada, and Zainal Arifin Ahmad. "Some ceramic properties of clays from central Cambodia." *Applied Clay Science* 53, no. 1 (2011): 33-41. https://doi.org/10.1016/j.clay.2011.04.017

[17] Standard, ASTM. "C373-88. Standard test method for water absorption, bulk density, apparent porosity and apparent specific gravity of fired whiteware products." *ASTM International, West Conshohocken, PA* (1999).

[18] Standard, ASTM. "C674-88. Standard Test Methods for Flexural Properties of Ceramic Whiteware Materials." *ASTM International, West Conshohocken, PA* (1999).

[19] Hajjaji, M., and H. El Arfaoui. "Adsorption of methylene blue and zinc ions on raw and acid-activated bentonite from Morocco." *Applied Clay Science* 46, no. 4 (2009): 418-421. https://doi.org/10.1016/j.clay.2009.09.010

[20] Bouazizi, A., S. Saja, B. Achiou, M. Ouammou, J. I. Calvo, A. Aaddane, and S. Alami Younssi. "Elaboration and characterization of a new flat ceramic MF membrane made from natural Moroccan bentonite. Application to treatment of industrial wastewater." *Applied Clay Science* 132 (2016): 33-40. https://doi.org/10.1016/j.clay.2016.05.009

[21] Huang, Weian, Y. Wang, Z. Qiu, Y-K. Leong, M. Cui, and H. Zhong. "Synthesis and characterisation of strong hydrophobic bentonite." *Materials Research Innovations* 19, no. 6 (2015): 428-434. https://doi.org/10.1179/1433075X15Y.0000000066

[22] Gridi-Bennadji, Fayza, G. Lecomte-Nana, Richard Mayet, Jean-Pierre Bonnet, and Sylvie Rossignol. "Effect of organic modification on the thermal transformations of abentonite during sintering up to 1250° C." *Bulletin of Materials Science* 38 (2015): 357-363. https://doi.org/10.1007/s12034-015-0876-1

[23] Ayari, F., E. Srasra, and M. Trabelsi-Ayadi. "Characterization of bentonitic clays and their use as adsorbent." *Desalination* 185, no. 1-3 (2005): 391-397. https://doi.org/10.1016/j.desal.2005.04.046

[24] Thommes, Matthias, Bernd Smarsly, Matthijs Groenewolt, Peter I. Ravikovitch, and Alexander V. Neimark. "Adsorption hysteresis of nitrogen and argon in pore networks and characterization of novel micro-and mesoporous silicas." *Langmuir* 22, no. 2 (2006): 756-764. https://doi.org/10.1021/la051686h

[25] Imoisili, Patrick E., Kingsley O. Ukoba, and Tien-Chien Jen. "Synthesis and characterization of amorphous mesoporous silica from palm kernel shell ash." *Boletín de la Sociedad Española de Cerámica y Vidrio* 59, no. 4 (2020): 159-164. https://doi.org/10.1016/j.bsecv.2019.09.006

[26] Kamoun, Naoufel, Fakher Jamoussi, and Miguel A. Rodríguez. "The preparation of meso-porous membranes from Tunisian clay." *Boletín de la Sociedad Española de Cerámica y Vidrio* 59, no. 1 (2020): 25-30. https://doi.org/10.1016/j.bsecv.2019.06.001

[27] WHO. "Recommendation 4nd edition." *World Health Organization, Geneva*, 2017.

[28] EPA. "National Primary Drinking Water Regulations." *EPA, US*, 2022. https://www.epa.gov/ground-water-and-drinking-water/national-primary-drinking-water-regulations.

[29] Kingsly, Tian Chee Cheah, and Jing Yao Sum. "Synthesis and evaluation of Fe-doped zinc oxide photocatalyst for methylene blue and congo red removal." *Progress in Energy and Environment* 22 (2022): 13-28. https://doi.org/10.37934/progee.22.1.1328